PalArch's Journal of Archaeology of Egypt / Egyptology

ANALYTICAL STUDY OF MICROPOLAR FLUID FLOW BETWEEN TWO POROUS DISKS

Reshu Agarwal
University of Petroleum and Energy Studies, Dehradun-248007
rgupta@ddn.upes.ac.in

Reshu Agarwal, Analytical Study of Micropolar Fluid Flow between Two Porous Disks-Palarch's Journal Of Archaeology Of Egypt/Egyptology 17(12), ISSN 1567-214x

Abstract

The present article analyzesthe axisymmetric steady, incompressible and laminar flow of a micropolar fluid between two parallel stationary disks with uniform porosity where both disks are subjected to uniform suction. In this study higher-order, nonlinear partial differential equations are reconstructed into a system of nonlinear ordinary differential equations by using Von Karman's similarity transformation. An analytical method,Homotopy Perturbation Method (HPM),is adopted to get the solution of obtained coupled nonlinear ordinary differential equations associated with boundary conditions. The behavior of the normal velocity, streamwise velocity components and the microrotation for severalparameters likesuction Reynolds number, vortex-viscosity, spin-gradient viscosity and micro-inertia densityhave been presented graphically. The validity of results obtained by HPM isverified by numerical results.The Maple software packageis usedfor calculation of velocity and the microrotation components.

Keywords

Porous Disks, Micropolar Fluid, Microrotation, Homotopy Perturbation Method, Numerical Method, Uniform Suction

1. Introduction

Eringen [1] presented the concept of simple microfluids which says that it is a medium whose properties and nature are affected by the fluid elements. This theory is updated by himself [2] and concluded a subclass of these fluids which are known as micropolar fluids. In the case of this fluid,two new velocity variables of micropolar fluidsare added which were not present in Navier-Stokes equations. The comprehensivestudy of micropolar fluids can be studied in the articles written by Eringen [3] and lukaszewicz [4].

The problem of the flow in the model of disks has a major field of interest in fluid mechanics. Such types of fluid flow have applications in hydrodynamical machines and apparatus, magnetic storage devices, crystal growth process etc. A Keller-box method was applied by Bhat and Katagi [5] to discuss the porosity of disks. MHD flow and heat transfer were investigated by Ashraf and Wehgal [6]. Agarwal and Dhanapal [7] [8], Takhar et al.[9] [10], Kamal et al. [11], Ashraf et al. [12] and Sajid et al. [13] have studiedthe flow and heat transfer of a micropolar fluid in different conditions of rotating disks by analytical and numerical methods. A shear flow problem for compressible viscous micropolar fluid numerically by Drazic et al [14]. Shabbir et al. [15] have studied modeling and numerical simulation of a micropolar fluid over a covered surfaced by the Keller-box method. Cattaneo-Christov heat flux model was studied by Doh et al. [16]. A numerical approach of partial slip effect in the flow of MHD micropolar nanofluid flow due to a rotating disk has been presented by Ramazan et al. [17]. Abbas et al. [18] have discussed an extended version of Yamada-ota

and Xu model. Khan et al. [19] have also discussed flow with modified Darcy's law.

The author has used an analytical approach to solve this model. Most of the flow problems are nonlinear. Some mathematicianshave solved a system of nonlinear ODEs numerically and some of them employed analytical methods to solve this type of equations. In this model authoremployed HPM to solve a system of non-linear ODEs and shown its comparison with a numerical method. Hojjati and Jafari [20], Bozkurt and Zuhal [21] have usedthe analytical technique to solve nonlinear problems in some models. He [22] has firstly developed the homotopy perturbation method in 1999. This method has been again updated by He [23-26]. The HPM is used in the flow past a rotating disk that has been discussed by Donald [27]. Jansi et al. [28] have discussed the analytical solution HPM to solve the model. Sheikholeslami et al. [29] have presented HPM for the three-dimensional problem. Recently, Agarwal and Mishra [30] and Agarwal [31] discussed flow and heat mass transfer in the rotating and stretchable disks respectively.

The primary objective of this article is to show the effect of different parameters on velocities and microrotation profiles in the present model. HPM is employed to solve nonlinear ODEs. To check the validity and exactness of the method, the results achieved by HPM are compared with the numerical method. The variation of streamwise velocity, normal velocity and microrotation profile has been discussed at different values of parameters and presented graphically.

2. Mathematical Formulation

Eringen [1] suggested thebasic equations of motion for thisfluid which are as follows:

$$\frac{\partial d}{\partial t} + \nabla(d\vec{V}) = 0 \qquad (1)$$

$$(\lambda + \mu + \kappa)\nabla(\nabla\vec{V}) - (\mu + \kappa)\nabla \times \nabla \times \vec{V} + \kappa\nabla \times \vec{\Omega} - \nabla p + d\,\vec{f} = d\frac{D\vec{V}}{Dt} \qquad (2)$$

$$(\alpha + \beta + \gamma)\nabla(\nabla.\vec{\Omega}) - \gamma(\nabla \times \nabla \times \vec{\Omega}) + \kappa\nabla\vec{V} - 2\kappa\vec{\Omega} + d\vec{c} = dj\frac{D\vec{\Omega}}{Dt} \qquad (3)$$

where $\vec{V}$ is the fluid velocity vector, $\vec{\Omega}$ is the microrotation, d is the density, p is the pressure, $\vec{f}$ and $\vec{c}$ are the body force and body couple per unit mass respectively.$\mu, d, j, \kappa, \gamma$are viscosity coefficients.$\frac{D}{Dt}$is the material derivative. The components of velocity and microrotation are given by

$$\vec{V} = \big(u_r(r,z), 0, u_z(r,z)\big), \qquad \vec{\Omega} = (0, \mathbb{N}(r,z), 0) \qquad (4)$$

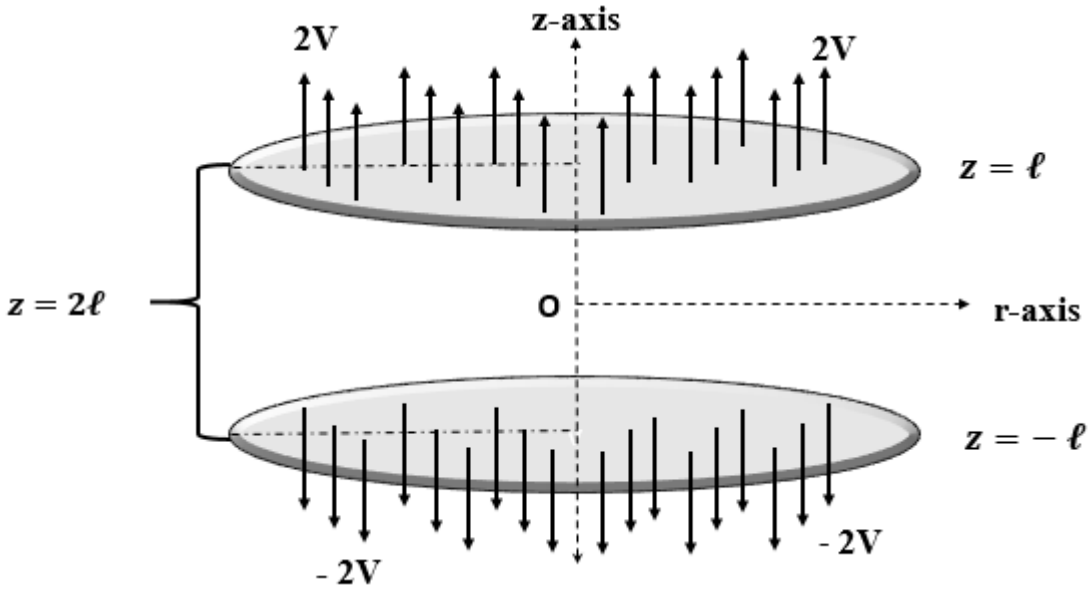

Fig (1) Model of the porous disks with uniform suction

In reference to cylindrical set (r, θ, z), let system has two infinite parallel disks stationed at $z = \pm\ell$. A micropolar fluid is occupied between these two parallel disks. We apply on the flow field a uniform suction with uniform velocity $2V$. Let the center of the disks is coinciding with the axis $r = 0$. We are also assuming the gap between both the disks (2ℓ) is less than to the radius of the disks. $u_r$andu_z are the components of the velocity in the direction of r-axis and z-axis respectively. $\mathbb{N}$is a microrotation of flow. Since uniform suction from both disks is considered in this model therefore the flow of fluid will be in an outward direction with uniform velocity $2V$. Since $curl\ \mathbb{N} = 0$ therefore, the component of microrotation will be considered zero.

On substituting velocity and microrotation vector in Eq (1)-Eq (3), we get the followingequations for such fluid which are as follows

$$\frac{\partial u_r}{\partial r} + \frac{u_r}{r} + \frac{\partial u_z}{\partial z} = 0 \tag{5}$$

$$u_r \frac{\partial u_r}{\partial r} + u_z \frac{\partial u_r}{\partial z} = \left(\frac{\mu+\kappa}{d}\right)\left(\frac{\partial^2 u_r}{\partial r^2} + \frac{1}{r}\frac{\partial u_r}{\partial r} - \frac{u_r}{r^2} + \frac{\partial^2 u_r}{\partial z^2}\right) - \frac{\kappa}{d}\frac{\partial \mathbb{N}}{\partial z} - \frac{1}{d}\frac{\partial p}{\partial r} \tag{6}$$

$$u_r \frac{\partial u_z}{\partial r} + u_z \frac{\partial u_z}{\partial z} = \left(\frac{\mu+\kappa}{d}\right)\left(\frac{\partial^2 u_z}{\partial r^2} + \frac{1}{r}\frac{\partial u_z}{\partial r} + \frac{\partial^2 u_z}{\partial z^2}\right) + \frac{\kappa}{d}\left(\frac{\partial \mathbb{N}}{\partial r} + \frac{\mathbb{N}}{r}\right) - \frac{1}{d}\frac{\partial p}{\partial z} \tag{7}$$

$$j\left(u_r \frac{\partial \mathbb{N}}{\partial r} + u_z \frac{\partial \mathbb{N}}{\partial z}\right) = \frac{\gamma}{d}\left(\frac{\partial^2 \mathbb{N}}{\partial r^2} + \frac{1}{r}\frac{\partial \mathbb{N}}{\partial r} - \frac{\mathbb{N}}{r^2} + \frac{\partial^2 \mathbb{N}}{\partial z^2}\right) + \frac{\kappa}{d}\left(\frac{\partial u_r}{\partial z} - \frac{\partial u_z}{\partial r}\right) - \frac{2\kappa\mathbb{N}}{d} \tag{8}$$

For both disks, boundary conditions (B.Cs.)may be written as

$$\left.\begin{array}{lllll} z=\ell: & u_r=0, & u_z=2V, & \mathbb{N}=0 \\ z=-\ell: & u_r=0, & u_z=-2V, & \mathbb{N}=0 \end{array}\right\}$$

(9)

Velocity field and microrotation field are required for solving problems, so we will solve Eq. (5)-Eq. (8) by using Eq. (5). Consider the following similarity transformation discussed by Karman [32]

$$\left.\begin{array}{l} u_r=-r\mathcal{F}'(z) \\ u_z=\ \ 2\mathcal{F}(z) \\ \mathbb{N}=\ -r\,\mathcal{G}(z) \end{array}\right\}$$

(10)

By using Eq. (10) in Eq. (5), we observe that similarity transformation satisfies the equation of continuity. Use Eq. (10) in Eq. (6) and Eq. (7) and after eliminating p, we get

$$(\mu+\kappa)\mathcal{F}^{iv}-\kappa\mathcal{G}''-2d\mathcal{F}\mathcal{F}'''=0$$

(11)

On putting Eq. (10) in Eq. (8), we get

$$\gamma\mathcal{G}''+\kappa\mathcal{F}''-2\kappa\mathcal{G}+dj(\mathcal{F}'\mathcal{G}-2\mathcal{F}\mathcal{G}')=0$$

(12)

Karman [30] introducedthe dimensionless variables which are as follows

$$f(\xi)=\frac{\mathcal{F}(z)}{V}, \qquad g(\xi)=\frac{\ell^2\mathcal{G}(z)}{V}$$

(13)

Where $\xi=\frac{z}{\ell}$ is a dimensionless parameter.

AfterusingEq. (13) in Eq. (11) and Eq. (12), we get

$$f^{iv}-\lambda_1 g''-2R_o f f'''=0$$

(14)

$$g'' + \lambda_2(f'' - 2g) - \lambda_3(2fg' - f'g) = 0 \quad (15)$$

Where $\lambda_1 = \frac{\kappa}{\mu+\kappa}$, $\lambda_2 = \frac{\kappa\ell^2}{\gamma}$, $\lambda_3 = \frac{dj\ell V}{\gamma}$, $R_o = \frac{dV\ell}{\mu+\kappa}$ are vortex viscosity, spin gradient viscosity, micro-inertia density parameter and suction Reynolds number respectively. Since R_o is proportional to V therefore $R_o > 0$ for suction and $R_o < 0$ for injection. $R_o > 0$has been considered in this study because of suction on both disks.

By using Eq. (9), Eq. (10) and Eq. (13),the following B.Cs are as follows

$$f(-1) = -1, \quad f'(-1) = 0, \quad g(-1) = 0,$$

$$f(1) = 1, \quad f'(1) = 0, \quad g(1) = 0 \quad (16)$$

To validate our model, we have to solve Eq (14) and Eq (15) by using boundary conditions (16).

3. Methodology

3.1Description of the Homotopy Perturbation Method

To explain the basic concepts, we study the following equation

$$A(u) - f(r) = 0, \quad r\epsilon\Omega \quad (17)$$

with the boundary conditions of

$$B\left(u, \frac{\partial u}{\partial n}\right) = 0, \quad r\epsilon\delta \quad (18)$$

Where $A(u)$ is a general differential operator, $f(r)$ is a known analytic function, B is a boundary operator and δ is a boundary of the domain Ω.

$A(u)$can be distributed into two parts where$L(u)$ is linear and $N(u)$ is non-linear.

ThereforeEq. (17) can be rewritten as

$$L(u) + N(u) - f(r) = 0, \qquad r\varepsilon\Omega \tag{19}$$

The HPM arrangement is as follows

$$H(v, \epsilon) = (1 - \epsilon)[L(v) - L(u_0)] + \epsilon[A(v) - f(r)] = 0 \tag{20}$$

Where $v(r, \epsilon): \Omega \times [0,1] \to R$ (21)

In Eq. (21), ϵ is an embedded parameter which lies between $[0,1]$ and u_0 is the first approximation that satisfies the B.Cs.

In the power of ϵ, solution of Eq. (20) can be written as

$$v = v_0 + \epsilon v_1 + \epsilon^2 v_2 + \ \ldots\ldots\ldots$$

And the best estimation for the solution is

$$u = \lim_{\epsilon \to 1} v = v_0 + v_1 + v_2 + \ \ldots\ldots\ldots$$

3.2 Application of Homotopy Perturbation Method

Initially define $P_1(f)$ and $P_2(g)$ for solving Eq. (14) and Eq. (15)

$$P_1(f) = f^{iv} - \lambda_1 g'' - 2R_o f f''' \tag{22}$$

$$P_2(g) = g'' + \lambda_2(f'' - 2g) - \lambda_3(2fg' - f'g) \tag{23}$$

Now divide $P_1(f)$ and $P_2(g)$ into two parts

$$L(f) + N(f) - U_1(r) = 0, \qquad L(g) + N(g) - U_2(r) = 0$$

Where $L(f), L(g)$ are linear parts and $N(f), N(g)$ are nonlinear parts of Eq. (14) and Eq. (15).

$$L(f) = f^{iv}, \qquad N(f) = -\lambda_1 g'' - 2R_o f f'''$$

(24)

$$L(g) = g'', \qquad N(g) = \lambda_2(f'' - 2g) - \lambda_3(2fg' - f'g)$$

(25)

By the homotopy technique, we construct a homotopy which satisfies

$$M_1(f, \epsilon) = (1 - \epsilon)\{L(f) - L(f_0)\} + \epsilon\{P_1(f) - U_1(r)\} = 0$$

(26)

$$M_2(g, \epsilon) = (1 - \epsilon)\{L(g) - L(g_0)\} + \epsilon\{P_2(g) - U_2(r)\} = 0$$

(27)

Where ϵ lies between 0 and 1. f_0, g_0arean initial approximation which satisfies boundary conditions and $U_1(r), U_2(r)$ are any analytical functions.

Now consider the approximate result of Eq. (26) and Eq. (27) in the power series as follows:

$$f(\xi) = \sum_{i=0}^{\infty} f_i \epsilon^i = f_0(\xi) + \epsilon f_1(\xi) + \epsilon^2 f_2(\xi) + \epsilon^3 f_3(\xi) + \ \ldots\ldots\ldots\ldots$$

(28)

$$g(\xi) = \sum_{i=0}^{\infty} g_i \epsilon^i = g_0(\xi) + \epsilon g_1(\xi) + \epsilon^2 g_2(\xi) + \epsilon^3 g_3(\xi) + \ \ldots\ldots\ldots\ldots$$

(29)

For the best approximation for a solution at $\epsilon \to 1$is

$$f(\xi) = f_0(\xi) + f_1(\xi) + f_2(\xi) + f_3(\xi) + \ \ldots\ldots\ldots\ldots$$

(30)

$$g(\xi) = g_0(\xi) + g_1(\xi) + g_2(\xi) + \ g_3(\xi) + \ \ldots\ldots\ldots\ldots$$

(31)

Using Eq. (24)-Eq. (29) and after simplification, we get

Coefficient of ϵ^0:

$$f_0{}^{iv} = 0, \tag{32}$$

$$g_0{}'' = 0 \tag{33}$$

Coefficient of ϵ^1:

$$f_1{}^{iv} - \lambda_1 g_0{}'' - 2R_o f_0 f_0{}''' = 0, \tag{34}$$

$$g_1{}'' + \lambda_2 (f_0{}'' - 2g_0) - \lambda_3 (2f_0 g_0{}' - f_0{}' g_0) = 0 \tag{35}$$

Coefficient of ϵ^2:

$$f_2{}^{iv} - \lambda_1 g_1{}'' - 2R_o (f_1 f_0{}''' + f_0 f_1{}''') = 0 \tag{36}$$

$$g_2{}'' + \lambda_2 (f_1{}'' - 2g_1) - \lambda_3 (2f_0 g_1{}' + 2f_1 g_0{}' - f_0{}' g_1 - f_1{}' g_0) = 0 \tag{37}$$

Coefficient of ϵ^3:

$$f_3{}^{iv} - \lambda_1 g_2{}'' - 2R_o (f_0 f_2{}''' + f_1 f_1{}''' + f_2 f_0{}''') = 0 \tag{38}$$

$$g_3{}'' + \lambda_2 (f_2{}'' - 2g_2) - \lambda_3 (2f_0 g_2{}' + 2f_1 g_1{}' + 2f_2 g_0{}' - f_0{}' g_2 - f_1{}' g_1 - f_2{}' g_0) = 0 \tag{39}$$

Solve Eq. (32)-Eq. (39) under the following boundary conditions:

$$\left.\begin{aligned} &f_0(-1) = -1,\ f_n(-1) = 0\ \forall n \geq 1,\quad f_n{}'(-1) = 0\ \ \forall n \geq 0,\ \ g_n(-1) = 0\ \ \forall n \geq 0 \\ &f_0(1) = 1,\quad f_n(-1) = 0\ \forall n \geq 1,\quad f_n{}'(1) = 0\ \ \forall n \geq 0,\quad g_n(1) = 0\ \ \forall n \geq 0 \end{aligned}\right\}$$

After simplification, we get

$$f_0(\xi) = \frac{1}{2}(-\xi^3 + 3\xi),$$

$$g_0(\xi) = 0,$$

$$f_1(\xi) = R_o\left(\frac{\xi^7}{280} - \frac{3\xi^5}{40} + \frac{39\xi^3}{280} - \frac{19\xi}{280}\right),$$

$$g_1(\xi) = \frac{\lambda_2}{2}(\xi^3 - \xi),$$

$$f_2(\xi) = -\frac{3{R_o}^2\xi^{11}}{30800} + \frac{{R_o}^2\xi^9}{420} - \frac{177{R_o}^2\xi^7}{9800} + \xi^5\left(\frac{17{R_o}^2}{700} + \frac{\lambda_1\lambda_2}{40}\right) - \frac{\xi^3}{6}\left(\frac{443{R_o}^2}{21560} + \frac{3\lambda_1\lambda_2}{10}\right) + \xi\left(\frac{\lambda_1\lambda_2}{40} - \frac{137{R_o}^2}{26950}\right).$$

$$g_2(\xi) = -\xi^7\left(\frac{\lambda_2\lambda_3}{56} + \frac{R_o\lambda_2}{280}\right) + \xi^5\left[\frac{3\lambda_2R_o}{40} + \frac{{\lambda_2}^2}{20} + \frac{7\lambda_2\lambda_3}{40}\right] - \xi^3\left[\frac{\lambda_2\lambda_3}{8} + \frac{117\lambda_2R_o}{840} + \frac{{\lambda_2}^2}{6}\right] + \xi\left[\frac{7{\lambda_2}^2}{60} - \frac{9\lambda_2\lambda_3}{280} + \frac{19R_o\lambda_2}{280}\right]$$

The value of $f_3(\xi)$ and $g_3(\xi)$ are too lengthy to be mention. So we will get the final value of $f(\xi)$ and $g(\xi)$ after substituting the values of f_i, g_i $(i = 0,1,2,3)$in the following equations,

$$f(\xi) = f_0(\xi) + f_1(\xi) + f_2(\xi) + f_3(\xi) + \ldots\ldots\ldots\ldots$$

$$g(\xi) = g_0(\xi) + g_1(\xi) + g_2(\xi) + g_3(\xi) + \ldots\ldots\ldots\ldots$$

To validate the present result of the study, the comparison between the results achieved by HPM and numerical results is done. The error of results for a specific value has been shown in Table 1-Table 3 which gives a good agreement between HPM and NM results. The comparison has been presented graphically in Fig (2)-Fig (4).

Table 1 Error of HPM and NM for $f(\xi)$ when $\lambda_1 = 1.5, \lambda_2 = 1.8, \lambda_3 = 1.2, R_o = 1$

ξ	HPM	NM	Error
1	-1	-1	0
-0.9	-0.9849986302	-0.9849002949	9.83353E-05
-0.8	-0.9420180521	-0.9417840931	0.000233959
-0.7	-0.8744112850	-0.8741901514	0.000221134
-0.6	-0.7857503592	-0.7857418041	8.5551E-06
-0.5	-0.6796226707	-0.6799502401	0.000327569
-0.4	-0.5594863165	-0.5601308161	0.0006445
-0.3	-0.4285817543	-0.4293864903	0.000804736
-0.2	-0.2898969571	-0.2906283121	0.000731355
-0.1	-0.1461812590	-0.1466147921	0.000433533
0	0.0000000000	0.0000000000	0.0000000000
0.1	0.1461812590	0.1466147921	0.000433533
0.2	0.2898969571	0.2906283121	0.000731355
0.3	0.4285817543	0.4293864903	0.000804736
0.4	0.5594863165	0.5601308161	0.0006445
0.5	0.6796226707	0.6799502401	0.000327569
0.6	0.7857503592	0.7857418041	8.5551E-06
0.7	0.8744112850	0.8741901514	0.000221134
0.8	0.9420180521	0.9417840931	0.000233959
0.9	0.9849986302	0.9849002949	9.83353E-05
1	1	1	0

Table 2 Error of HPM and NM for $f'(\xi)$ when $\lambda_1 = 1.5, \lambda_2 = 1.8, \lambda_3 = 1.2, R_o = 1$

ξ	HPM	NM	Error
-1	0	0	7.3E-18
-0.9	0.2951932149	0.296756783	0.001563568
-0.8	0.5587856394	0.559608974	0.000823334
-0.7	0.7873624795	0.786199699	0.001162781
-0.6	0.9798529871	0.976902394	0.002950593
-0.5	1.1369226246	1.133401224	0.003521401
-0.4	1.2603979986	1.25781949	0.002578508
-0.3	1.3527157853	1.352222072	0.000493713
-0.2	1.4164073120	1.418352117	0.001944805
-0.1	1.4536454581	1.45750351	0.003858051
0	1.4658874599	1.470465722	0.004578262
0.1	1.4536454581	1.45750351	0.003858051
0.2	1.4164073120	1.418352117	0.001944805
0.3	1.3527157853	1.352222072	0.000493713
0.4	1.2603979986	1.25781949	0.002578508
0.5	1.1369226246	1.133401224	0.003521401
0.6	0.9798529871	0.976902394	0.002950593
0.7	0.7873624795	0.786199699	0.001162781
0.8	0.5587856394	0.559608974	0.000823334
0.9	0.2951932149	0.296756783	0.001563568
1	0	0	7.3E-18

Table 3 Error of HPM and NM for $g(\xi)$ when $\lambda_1 = 1.5, \lambda_2 = 1.8, \lambda_3 = 1.2, R_o = 1$

ξ	HPM	NM	Error
-1	0	0	6.7E-18
-0.9	0.1554935842	0.157088996	0.001595412
-0.8	0.2381682428	0.240666167	0.002497924
-0.7	0.2725667090	0.274147109	0.0015804
-0.6	0.2750542429	0.273949253	0.00110499
-0.5	0.2559607144	0.251355968	0.004604747
-0.4	0.2216035509	0.214031097	0.007572454
-0.3	0.1759852735	0.167164678	0.008820595
-0.2	0.1220499366	0.114305126	0.00774481
-0.1	0.0624686661	0.057954454	0.004514213
0	0.0000000000	0.0000000000	0.0000000000
0.1	-0.0624686661	-0.057954454	0.004514213
0.2	-0.1220499366	-0.114305126	0.00774481
0.3	-0.1759852735	-0.167164678	0.008820595
0.4	-0.2216035509	-0.214031097	0.007572454
0.5	-0.2559607144	-0.251355968	0.004604747
0.6	-0.2750542429	-0.273949253	0.00110499
0.7	-0.2725667090	-0.274147109	0.0015804
0.8	-0.2381682428	-0.240666167	0.002497924
0.9	-0.1554935842	-0.157088996	0.001595412
1	0	0	6.7E-18

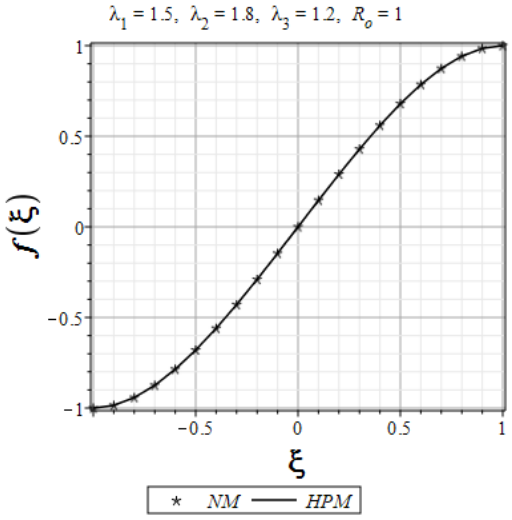

Fig (2) Comparative graph of NM and HPM for $f(\xi)$

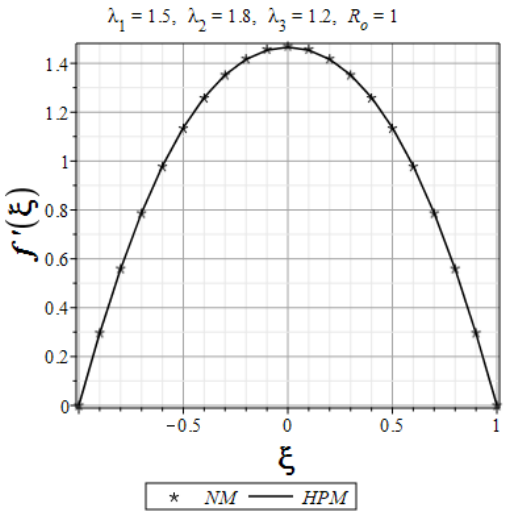

Fig (3) Comparative graph of NM and HPM for $f'(\xi)$

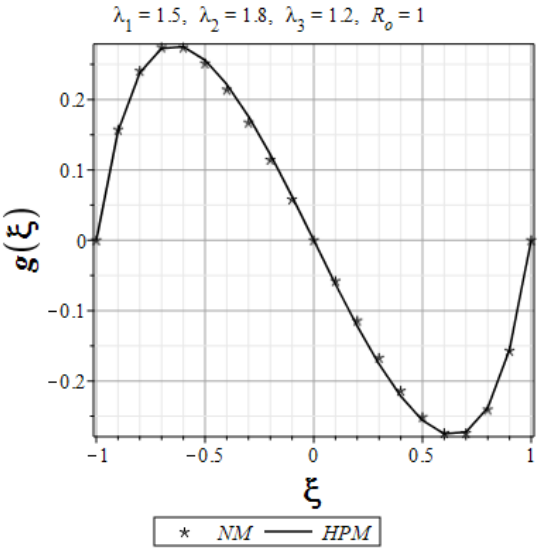

Fig (4) Comparative graph of NM and HPM for $g(\xi)$

4. Results and Discussion

The behavior of $f(\xi)$, $f'(\xi)$ and $g(\xi)$ at the several values of suction Reynolds number (R_o), vortex viscosity (λ_1), spin-gradient viscosity (λ_2) and microrotation density (λ_3) are discussed in Fig (5)-Fig (16).

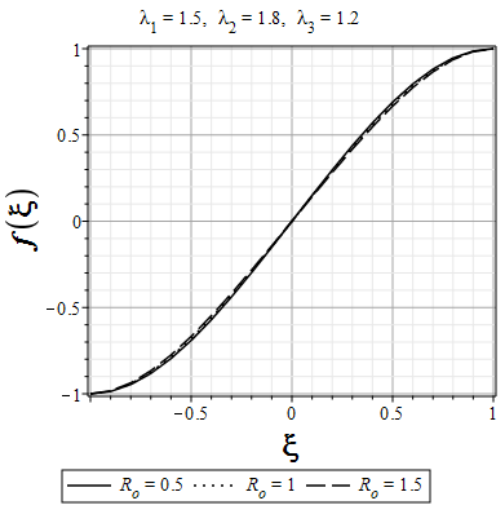

Fig (5) $f(\xi)$ for several values ofR_o

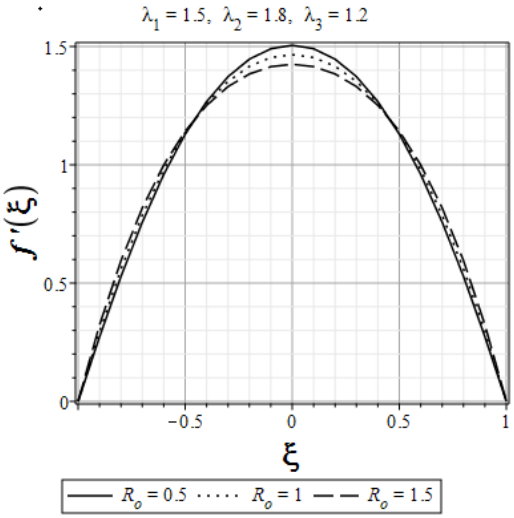

Fig (6) $f'(\xi)$for several values of R_o

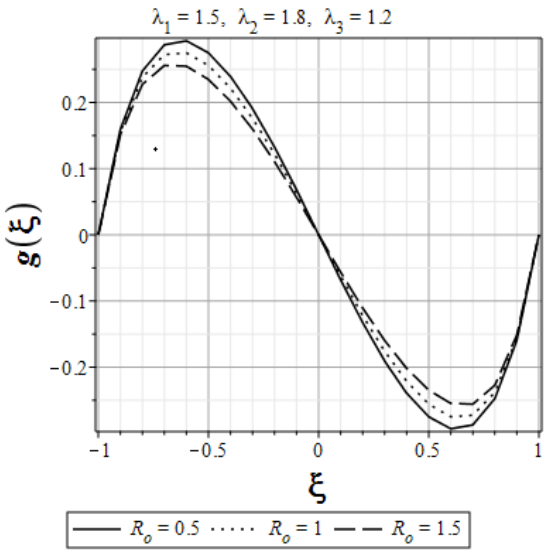

Fig (7) $g(\xi)$for several values of R_o

The influence of different values of suction Reynold number $R_o = 0.5, 1, 1.5$when $\lambda_1 = 1.5, \lambda_2 = 1.8, \lambda_3 = 1.2$ on the flow velocities and microrotation profile are investigated in Fig (5)-Fig (7). Fig (5) depicts that normal velocity increases with an increase in R_o near the lower disk while it decreases with an increase in R_o near the upper disk. It can also be observed that normal velocity reaches its value 1 at the upper disk and decreases to -1 at the lower disk. Also, normal velocity changes its concavity near $z = 0$. Fig (6) investigates that $f'(\xi)$ follows a parabolic path. Also, it increases near both disks with an increase in R_o while near the central plane it decreases with an increase in R_o. It can also be noted that streamwise velocity achieves its maximum at the central plane. Fig (7) depicts that microrotation decreases with an increase in R_o near the lower disk while it increases with an increase in R_o near the upper disk.Also, its behavior is symmetric and reversed along $z = 0$.

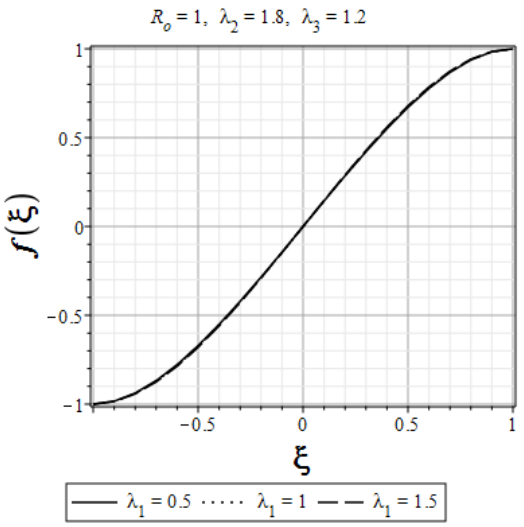

Fig (8) $f(\xi)$for various values ofλ_1

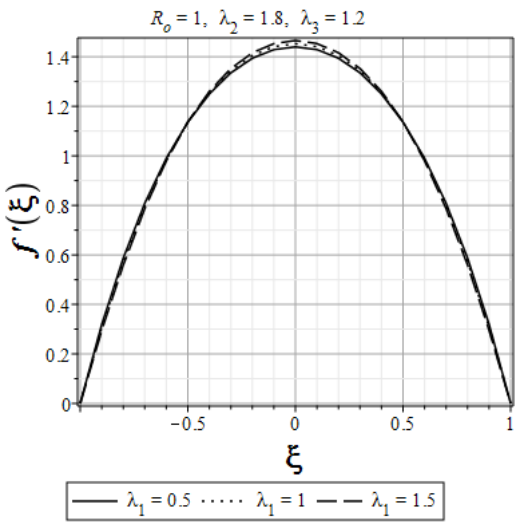

Fig (9) $f'(\xi)$for various values of λ_1

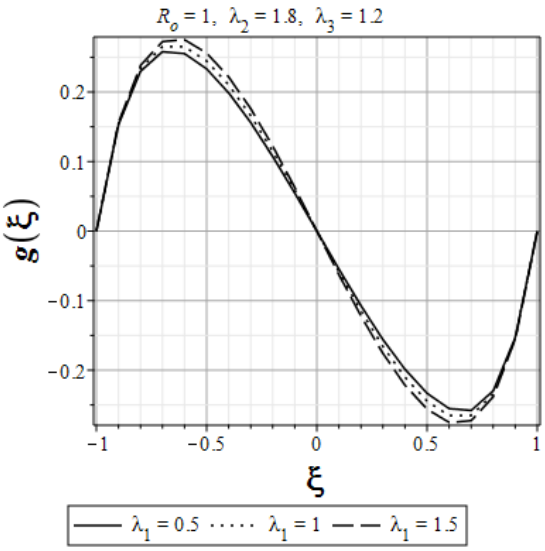

Fig (10) $g(\xi)$for various values of λ_1

Fig (8)-Fig (10) display the effect of various values of the vortex viscosity parameter $\lambda_1 = 0.5, 1, 1.5$ when $R_o = 1, \lambda_2 = 1.8, \lambda_3 = 1.2$on $f(\xi)$, $f'(\xi)$ and $g(\xi)$ respectively. Fig (8) shows no significant change in normal velocity for different values of λ_1. Fig (9) indicates the behavior of streamwise velocity $f(\xi)$. A parabolic nature in the velocity component can be seen from this figure. Near both disks, a small decrement in magnitude can also be observed with an increase in vortex viscosity parameter (λ_1). But near the central plane $(z = 0)$ streamwise velocity $(f'(\xi))$ increases with an increase in λ_1. Fig (10) shows that

microrotation increases near the lower disk while it decreases near the upper disk with an increase in λ_1.

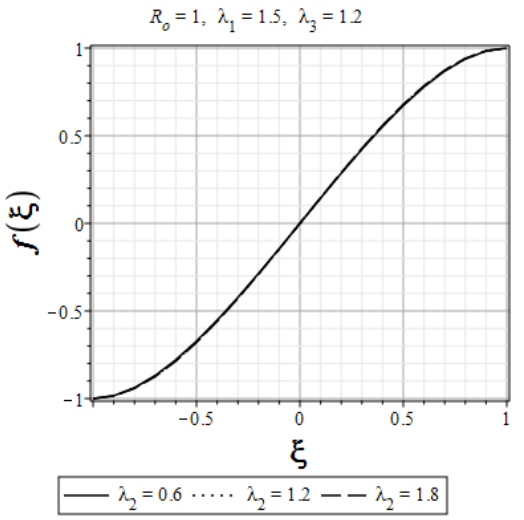

Fig (11) $f(\xi)$for various values of λ_2

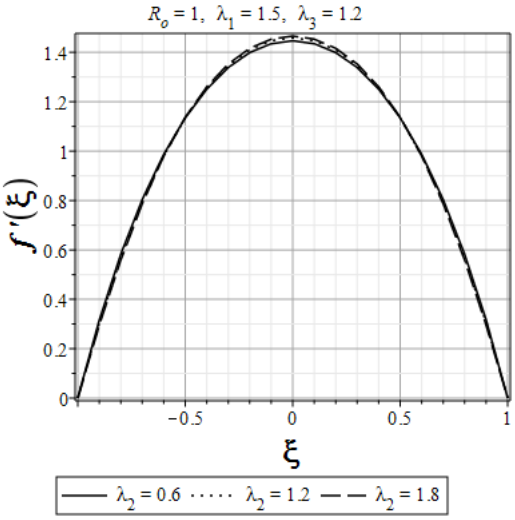

Fig (12) $f'(\xi)$for various values of λ_2

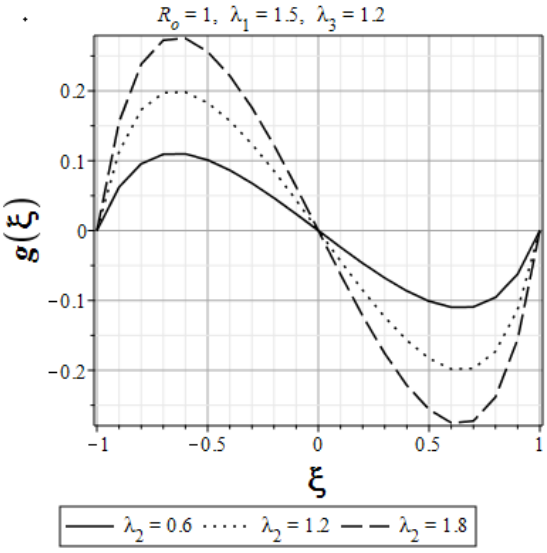

Fig (13) $g(\xi)$for various values of λ_1

Fig (11)-Fig (13) display the influence of λ_2 on both velocity component and microrotation profile. Fig (11) shows that there is no significant change in $f(\xi)$ by changing spin-gradient viscosity λ_2. Fig (12) investigates that $f'(\xi)$ decreases with an increase in λ_2 near both disks, while near $z = 0$, velocity increases with an increase in λ_2. Fig (13) displays the behavior of microrotation $g(\xi)$ which

tells that near the lower disk microrotation increases with an increase in λ_2 whereas its behavior is reversed near the upper disk.

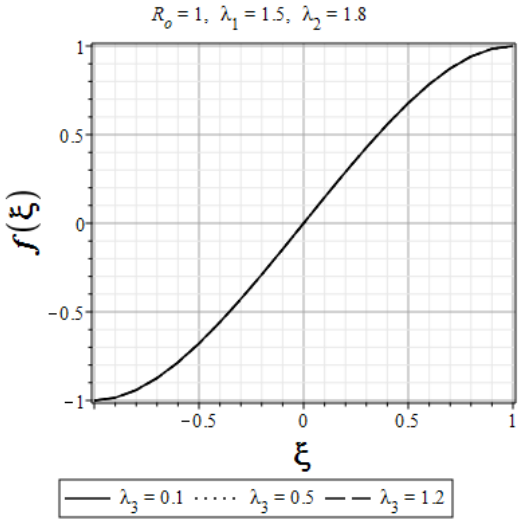

Fig (14) $f(\xi)$for various values of λ_3

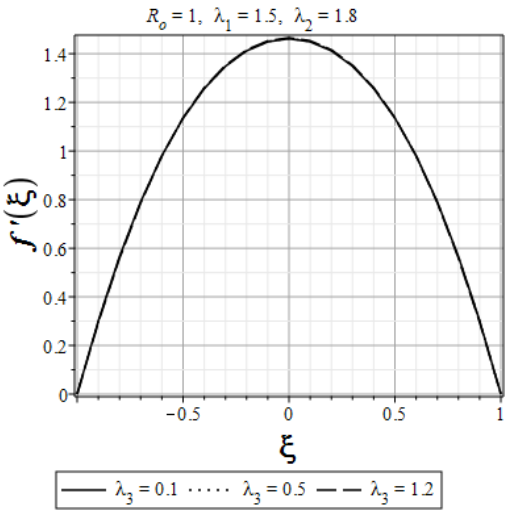

Fig (15) $f'(\xi)$for various values of λ_3

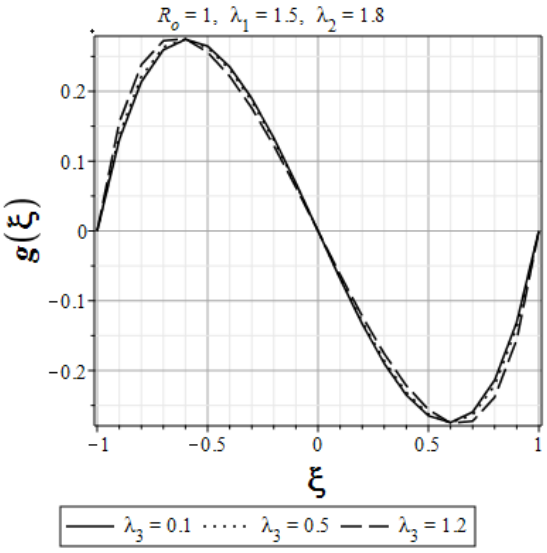

Fig (16) $g(\xi)$for various values of λ_3

Fig (14)-Fig (16) depict the effect of the microrotation density parameter λ_3 on $f(\xi), f'(\xi)$ and $g(\xi)$ respectively. Fig (14) shows that no change in $f(\xi)$on changing λ_3. Fig (15) investigates the parabolic behavior of $f'(\xi)$. Also,$f'(\xi)$ has no change in varying λ_3. Fig (16) investigates that the behavior of the microrotation profile is symmetric but opposite along the central plane $z = 0$. It is clear from this figure that $g(\xi)$ increases with an increase in λ_3 near the lower

disk while near the central plane $g(\xi)$ decreases with an increase in λ_3. Its behavior is reversed near the upper disk.

5. Conclusion

In this paper, micropolar fluid flow between two porous disks is solved by HPM. The obtained results are compared with numerical results. The author makes the following conclusion:

- The performance of normal, streamwise velocities and the microrotation are similar for various parameters.
- The streamwise velocity escalates at the points which are nearby$z = 0$ with an increase in vortex-viscosity (λ_1), spin-gradient viscosity (λ_2), micro-inertia density (λ_3).
- The streamwise velocity falls nearby$z = 0$ with a rise in suction Reynolds number R_o.
- Results show an acceptable agreement between HPM results and numerical method results.
- The error shows that HPM is a better approach for solving nonlinear ordinary differential equations.

Conflict of Interest

There is no conflict of interest.

References

1. A. C. Eringen. Simple microfluids. Int. J. Engg. Sci.2 (1964) 205-217.
2. A. C. Eringen. Theory of micropolar fluids. J. Math. Mech.16 (1966) 1-18.
3. A. C. Eringen. Micro continuum fields theories-II.Springer, New York2001.
4. Lukaszewicz G. Micropolar fluids: theory and application. *Boston.* 1999.

5. Bhat Ashwani and Nagaraj N. Katagi. Micropolar fluid flow between a non-porous disk and a porous disk with slip by Keller box method. Ain Shams Engg. J.11 **(**2020) 149-159.
6. Ashraf M. and A. R. Wehgal. MHD flow and heat transfer of micropolar fluid between two porous disks. Applied Mathematics and Mechanics.33 (2012) 51-64.
7. Agarwal R. S. and C. Dhanapal. Stagnation point of micropolar fluid flow between porous discs with uniform blowing. Int. J. of Engg. Sci.26 (1988) 293-300.
8. Agarwal R. S. and C. Dhanapal. Numerical solution of a micropolar fluid flow between a rotating and a porous stationary disk. Int. J. of Engg. Sci.25 (1987) 1403-1417.
9. Takhar H. S., R. Bhargava and R. S. Agarwal. Finite element solution of micropolar fluid flow from an enclosed rotating disk with suction and injection. Int. J. of Engg. Sci.39 (2001) 913-927.
10. Takhar H. S., R. S. Agarwal, R. Bhargava and V. M. Soundalgekar. Flow of a micropolar fluid past a decelerating porous rotating disk. Int. J. Non-linear Mechanics.30 (1995) 295-304.
11. Kamal M. A., M. Ashraf and K. S. Sayed. Numerical solution of steady viscous flow of a micropolar fluid driven by injection between two porous disks. Applied Mathematics and Computation. 179 (2006) 1-10.
12. Ashraf M., M. A. Kamal and K. S. Sayed. Numerical simulation of flow of a micropolar fluid between a porous disk and a non-porous disk.Applied Mathematical Modelling.33 (2009) 1933-43.

13. Sajid M., M. N. Sadiq, N. Ali and T. Javed. Numerical simulation for Homann flow of a micropolar fluid on a spiralling disk. European J. of Mechanics/B Fluids.72 (2018) 320-7.
14. Drazic Ivan, Nelida Crnjaric-Zic and Loredana Simcic. A shear flow problem for compressible viscous micropolar fluid deviation of the model and numerical solution. Mathematics and Computers in Simulation.162 (2019) 249-67.
15. Shabbir T., M. Mushtaq, M. Ijazkan and T. Hayat. Modelling and numerical simulation of micropolar fluid over a covered surfaced by Keller-box method. Computer Methods and Programs in Biomedicine.187 (2020) 105220.
16. Doh Deag-Hee, Gyeong-Rae Cho, E. Ramya and M. Muthtamilselvan. Cattaneo-Christov heat flux model for inclined MHD micropolar fluid flow past a non-linearly stretchable rotating disk. Case Studies in Thermal Engg.14 (2019) 100496.
17. Ramazan M. Jae Dong Chaung and Naeen Ullah. A numerical approach of partial slip effect in the flow of MHD micropolar nanofluid flow due to a rotating disk. Results in Physics.7 (2017) 3557-66.
18. Abbas Nadeem, S. Nadeem and M. Y. Malik. An extended version of Yamada-ota and Xu model in micropolar fluid flow under the region of stagnation point. Physica A Statistical Mechanics and its application.542 (2020) 123512.
19. Khan N. A., S. Khan and A. Ara. Flow of a micropolar fluid over an off centred rotating disk with modified Darcy's law. Propulsion and Power Research.6 (2017) 285-95.
20. Hojjati M. M. and S. Jafari. Semi exact solution of elastic non-uniform thickness and density rotating disk by homotopy perturbation method and adomian decomposition method. Int. J. of Pressure Vessels and Piping.85 (2008) 871-8.

21. Bozkurt S. and Zuhal Elif Khan.axisymmetric deformation analysis of thick-walled cylinder and rotating disks using improved ADM. Int. J. of Mechanics.12 (2018) 14-8.
22. He J. H. Recent developments of the Homotopy perturbation methods. Top Methods Non-linear Analysis.31 (2008) 205-209.
23. He J. H. Homotopy perturbation method for solving boundary value problems. Phys. Lett. A.350 (2006) 87-8.
24. He J. H. Comparison of Homotopy perturbation method and Homotopy Analysis Method. Appl. Math. Computation.156 (2004) 527-39.
25. He J. H. A coupling method of a homotopy technique and perturbation technique for non-linear problems. Int. J. Non-linear Mech.35 (2000) 37-43.
26. He J. H. Homotopy perturbation technique.Comp. Math. App. Mech. Engg.178 (1999) 257-62.
27. Donald P. Ariel. The HPM and analytical solution of the problem of the flow past a rotating disk. Computer and Mathematics in Applications.58 (2009) 2504-13.
28. Jansi P. G., M. Kirthiga, Angela Molina and E. Laborda. Analytical solution of the convection diffusion equation for uniformly accessible rotating disk electrodes via the HPM. J. of Electrolytical Chemistry.799 (2017) 175-180.
29. Sheikholeslami M., H. R. Ashorynejad, D. D. Ganji and A. Yildirim. HPM for three dimensional problem of condensation fluid on inclined rotating disk. Scientia Iranica.19 (2012) 437-442.
30. Agarwal R. and Mishra P. Analytical Solution of the MHD Forced Flow and Heat Transfer of a non-Newtonian Visco-Inelastic Fluid between Two Infinite Rotating Disks. Materials Today: Proceeddings. https://doi.org/10.1016/j.matpr.2020.10.632.

31. Agarwal R. Heat and mass transfer in electrically conducting micropolar fluid flow between two stretchable disks. Materials Today: Proceeddings. https://doi.org/10.1016/j.matpr.2020.11.614.
32. Von Karman T. Under laminare and turbulence Reibung. Z. Angew Math. Mech. 1 (1921) 233-5.